

Electronic Supplementary Information (ESI) for

Fabrication of a One-dimensional Tube-in-tube Polypyrrole/Tin oxide Structure for Highly Sensitive DMMP Sensor Applications

Jaemoon Jun, Jun Seop Lee, Dong Hoon Shin, Jungkyun Oh, Wooyoung Kim, Wonjoo Na, and Jyongsik Jang *

School of Chemical and Biological Engineering, College of Engineering, Seoul National University (SNU), 599 Gwanangno, Gwanak-gu, Seoul, 151-742 (Korea). Fax: +82-2-888-7295; Tel: 82-2-880-8348; e-mail: jsjang@plaza.snu.ac.kr

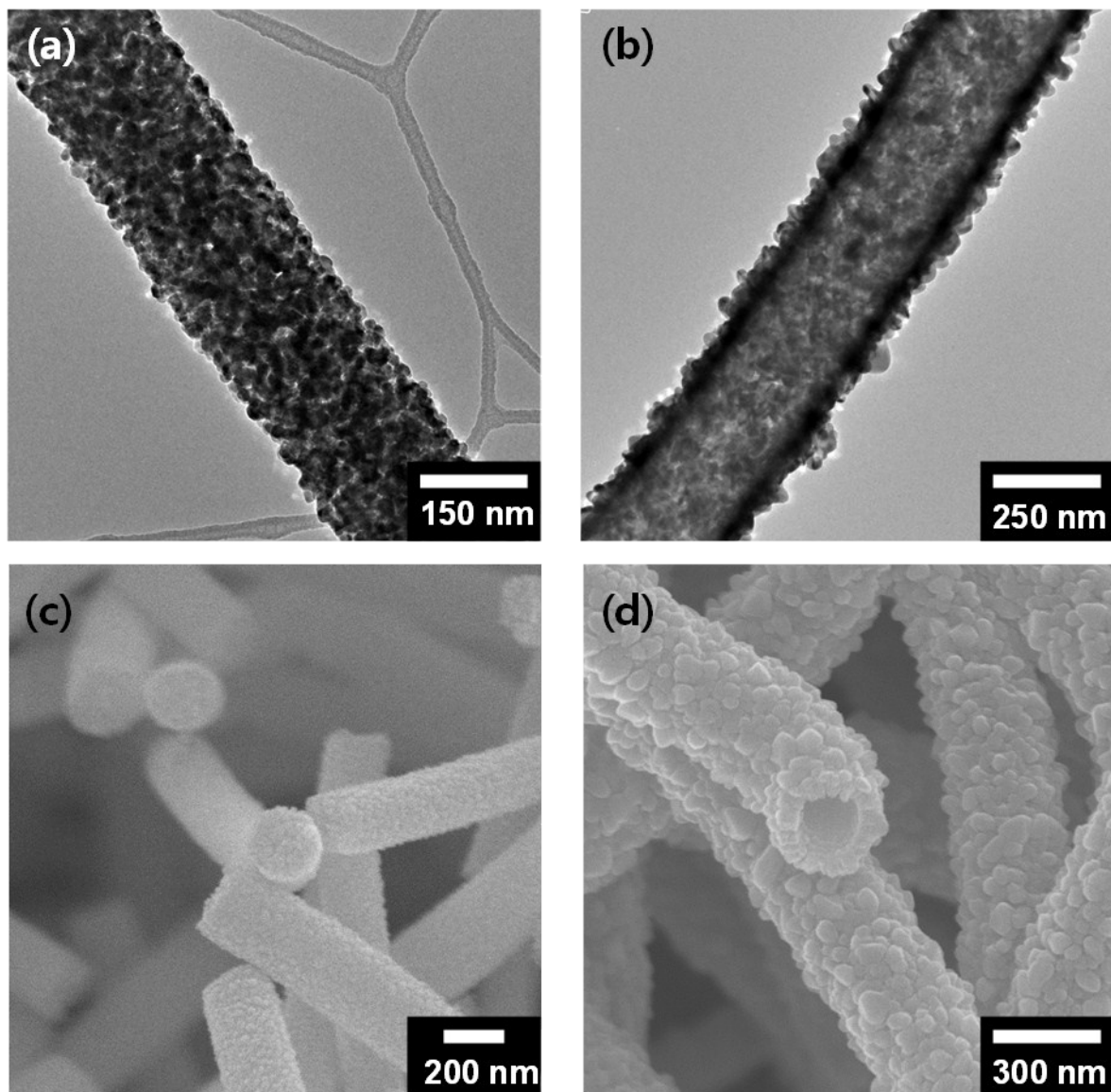


Fig. S1. (a, c) Transmission electron microscopy (TEM) and scanning electron microscopy (SEM) images of the SnO₂ fibers. (b, d) TEM and SEM images of the SnO₂ tubes.

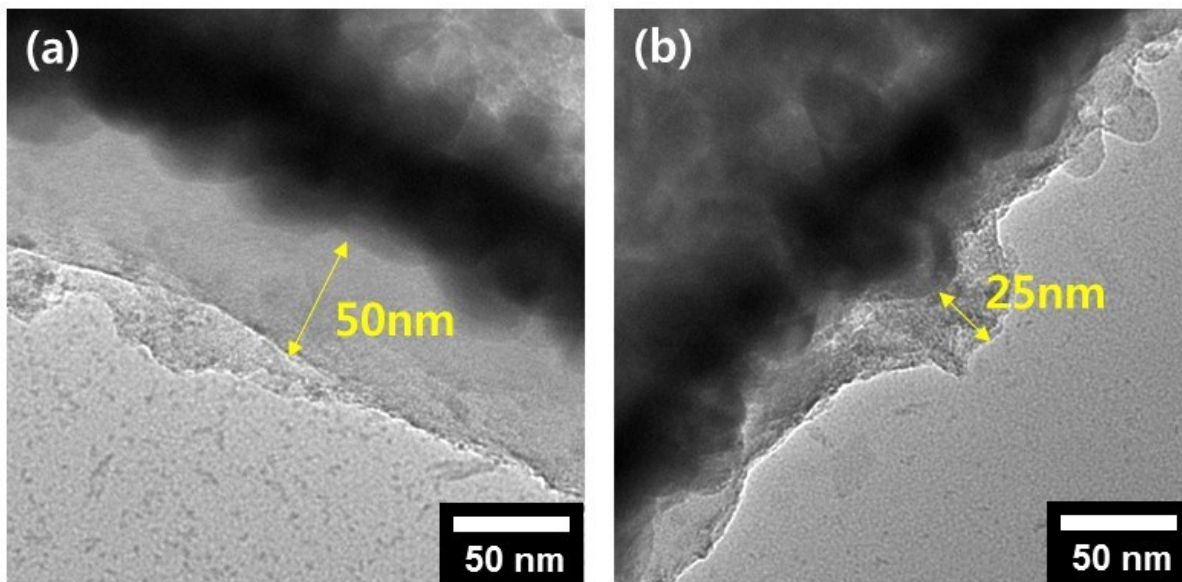


Fig. S2. Transmission electron microscopy (TEM) images of the PPy@SnO₂ tube in tube by conducting the VDP step at different temperature (a)60°C and (b)100°C.

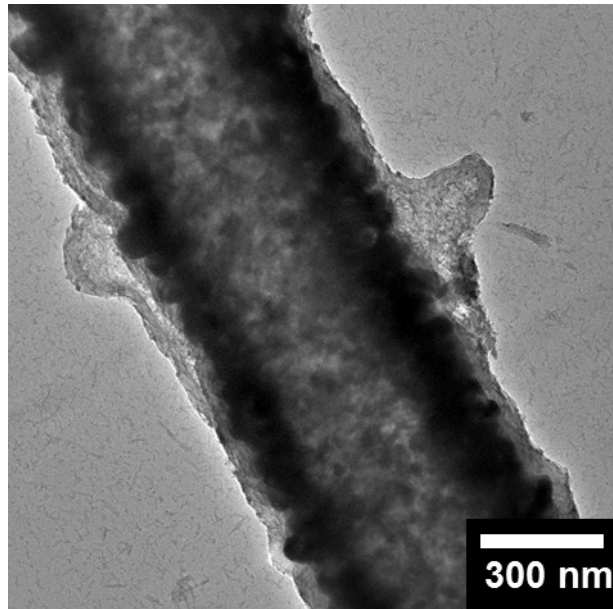


Fig. S3. TEM image of the morphology of the PPY coated SnO₂ tube structure after VDP method in ambient state.

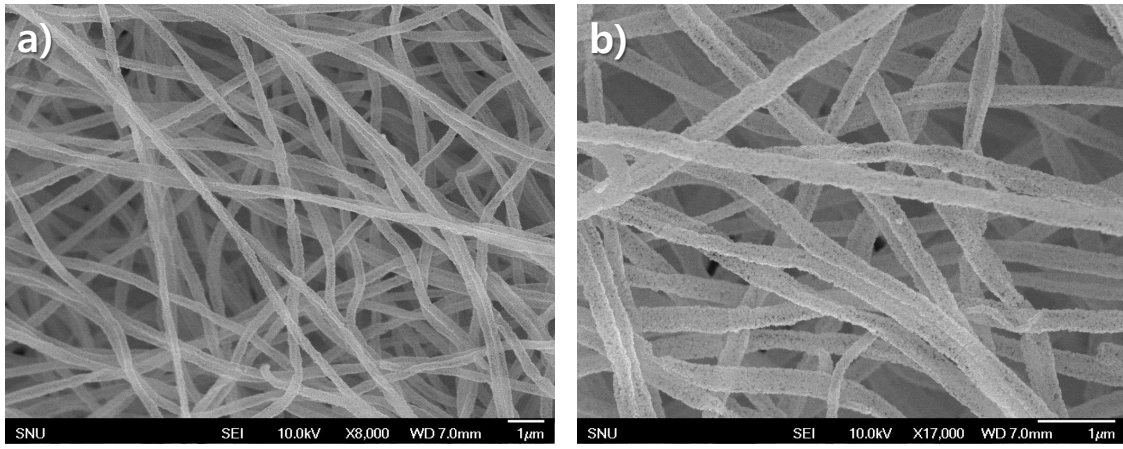


Fig. S4. (a) Low-and (c) high-resolution FE-SEM images of the tube-in-tube SnO₂.

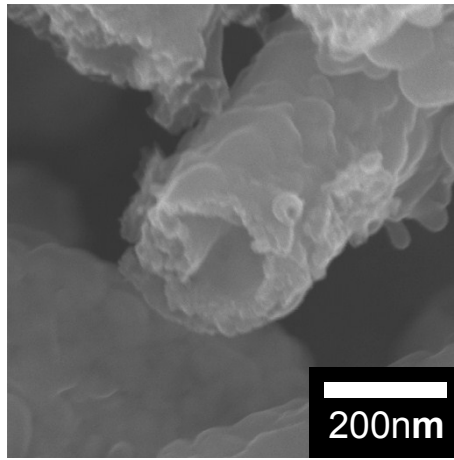


Fig. S5. High-resolution SEM image of the PPy@SnO₂ tube in tube.

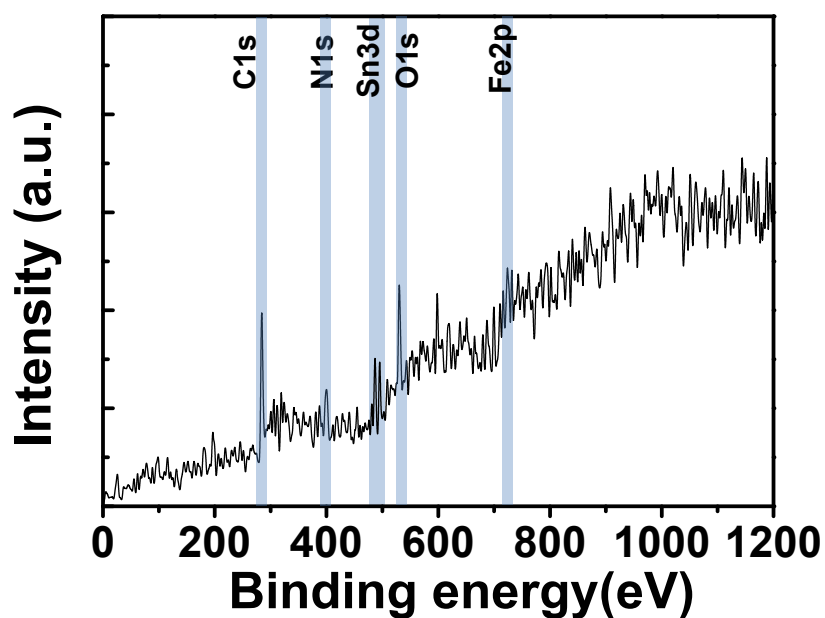


Fig. S6. . X-ray photoelectron spectroscopy (XPS) analysis of a fully scanned spectra (0–1200 eV).

Fig.S6 shows the overall XPS spectroscopy of the PPy@SnO₂ tube in tube over the range of 0-1200eV; carbon, nitrogen, oxygen, tin, and iron atoms were present. Based on the XPS peak, it is considered that the small quantities of iron atom originated from FeCl₃ solution is still exist.

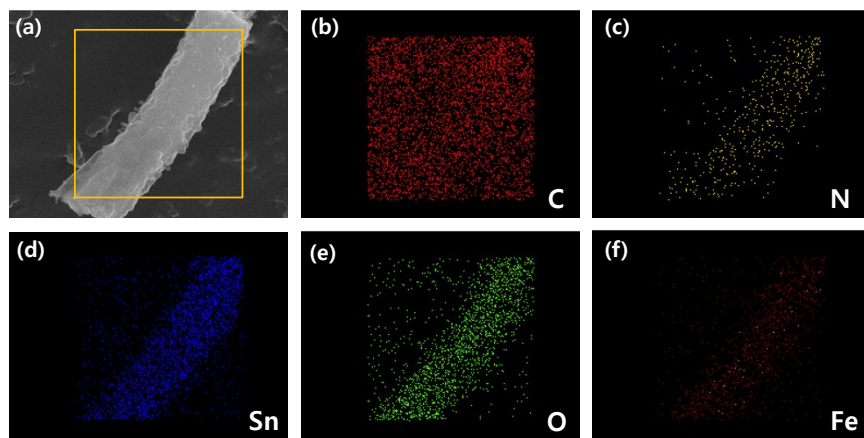


Fig. S7. EDS dot mapping of PPy@SnO₂ tube in tube surface components indicating (a) overall SEM image, (b) carbon, (c) nitrogen, (d) tin, (e) oxygen and (f) iron

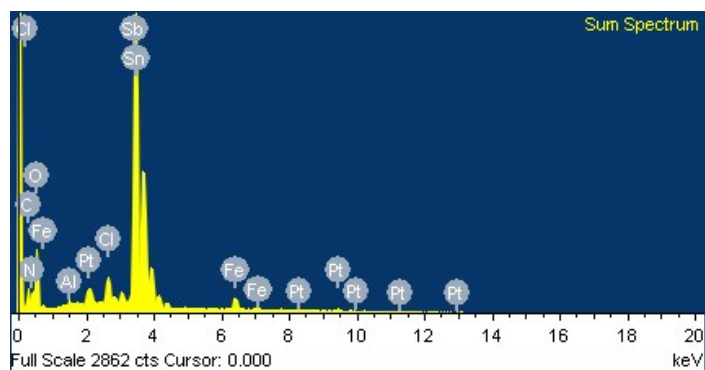


Fig. S8. EDX spectrum of the PPy@SnO₂ tube in tube surface

Table S1. Summarized elemental distribution of the PPy@SnO₂ tube in tube

Element	Weight%	Atomic%
CK	5.42	14.30
NK	5.64	12.77
OK	27.71	54.94
AlK	0.31	0.36
ClK	1.50	1.35
FeK	2.15	1.22
SnL	51.54	13.77
SbL	3.66	0.95
PtM	2.07	0.34

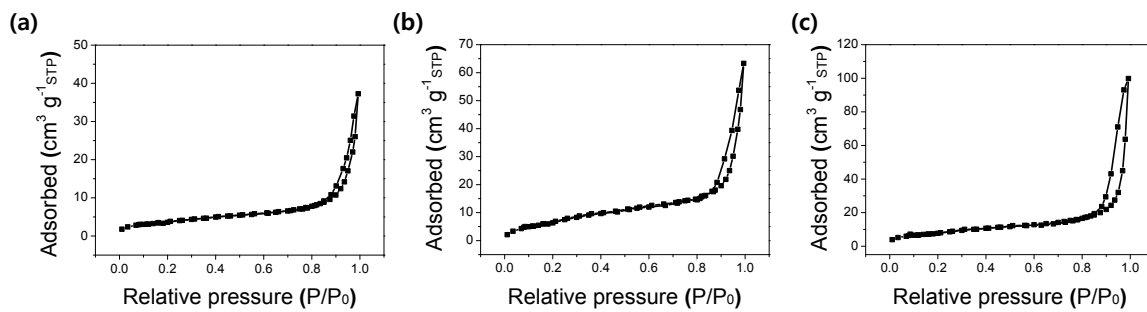


Fig. S9. Nitrogen adsorption–desorption isotherm curves of (a) Fiber, (b) Tube, and (c) Tube-in-tube.

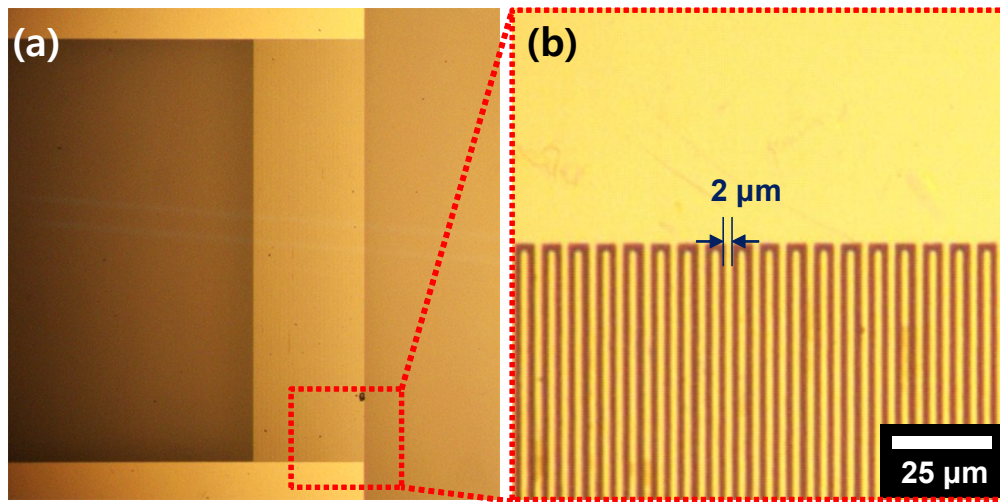


Fig. S10. (a) Low- and (b) high-resolution optical microscopy images of the interdigitated array (IDA) electrode.

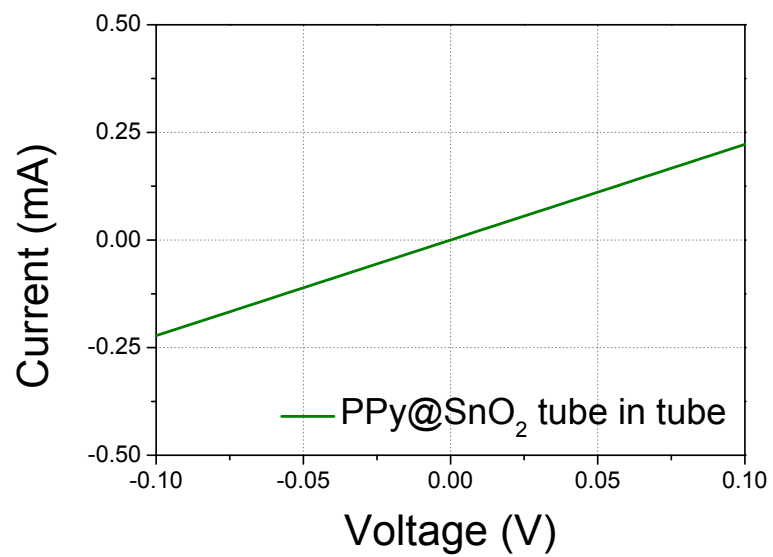


Fig. S11. Current–voltage ($I-V$) curve of the tube-in-tube PPy@SnO₂ sensor electrode.

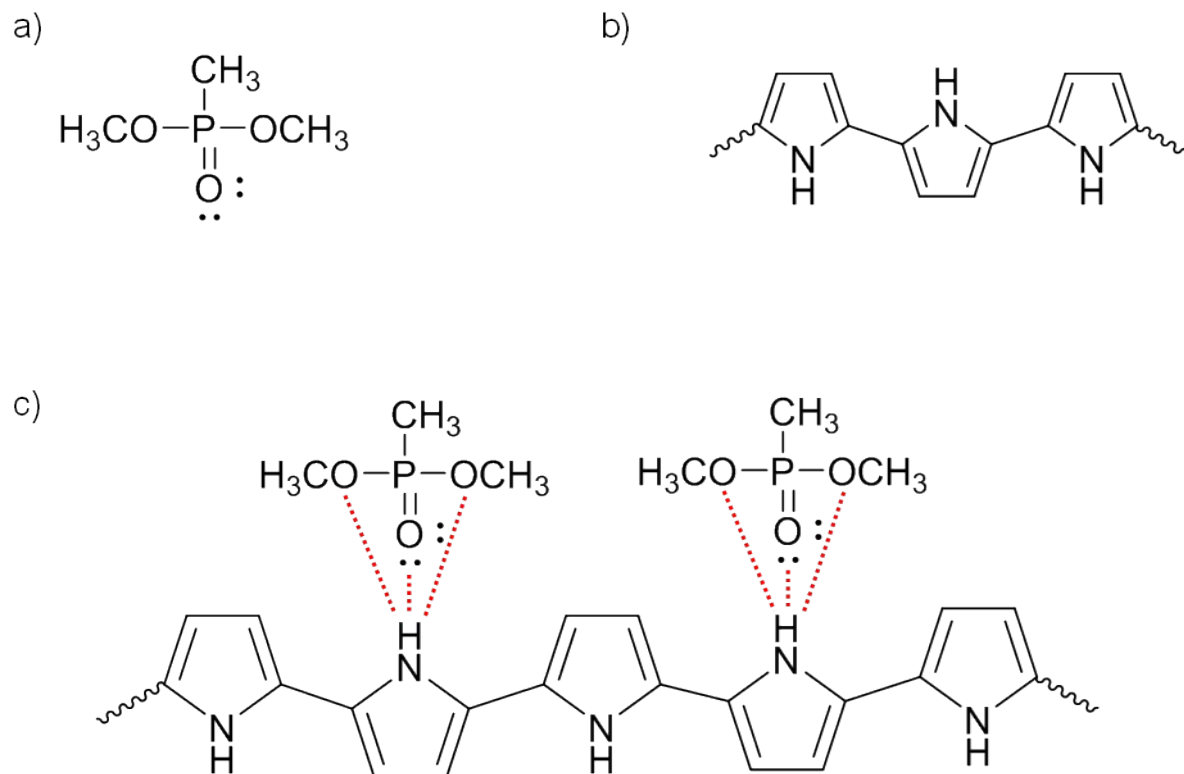


Fig. S12. Molecular structures of (a) dimethyl methylphosphonate (DMMP) and (b) polypyrrole (PPy).
 (c) Schematic diagram describing the effect of hydrogen bonding on PPy.

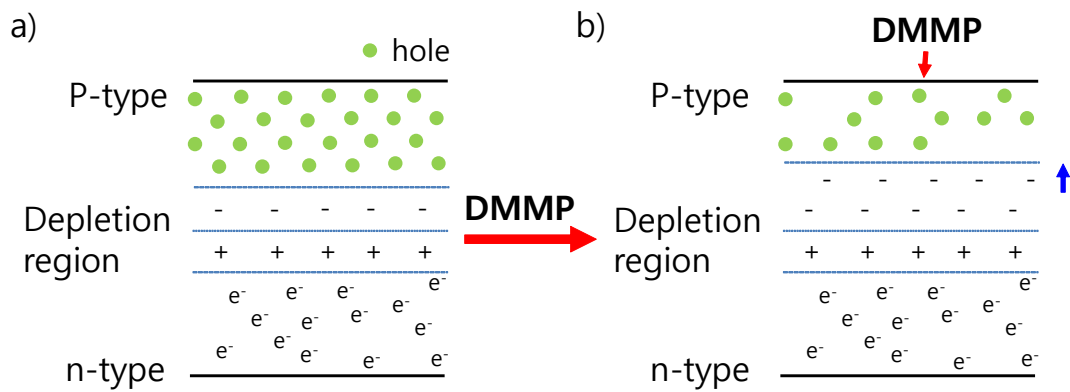


Fig. S13. Schematic diagram of the formation of a p-n junction.

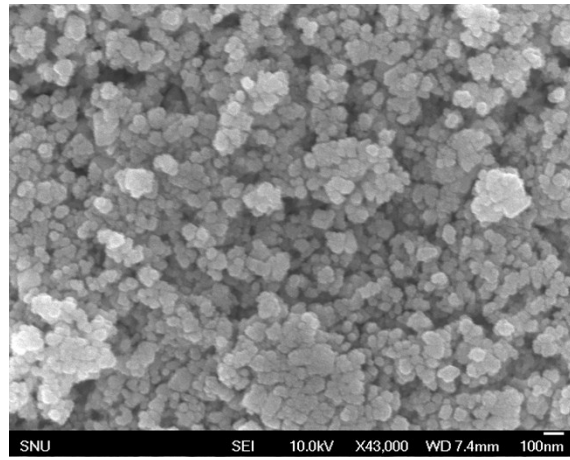


Fig. S14. SEM image of the PPy@SnO₂ nanoparticles.

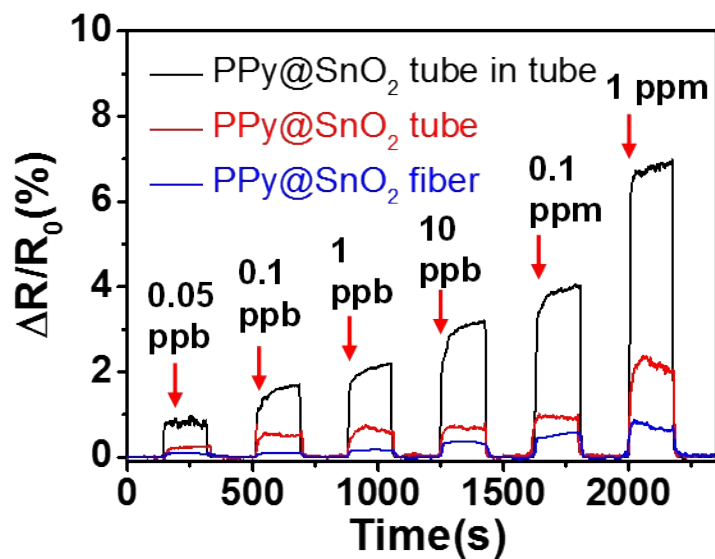


Fig. S15. Real-time monitoring of PPy@SnO₂ having different one-dimensional (1D) structures after sequential exposure to DMMP.

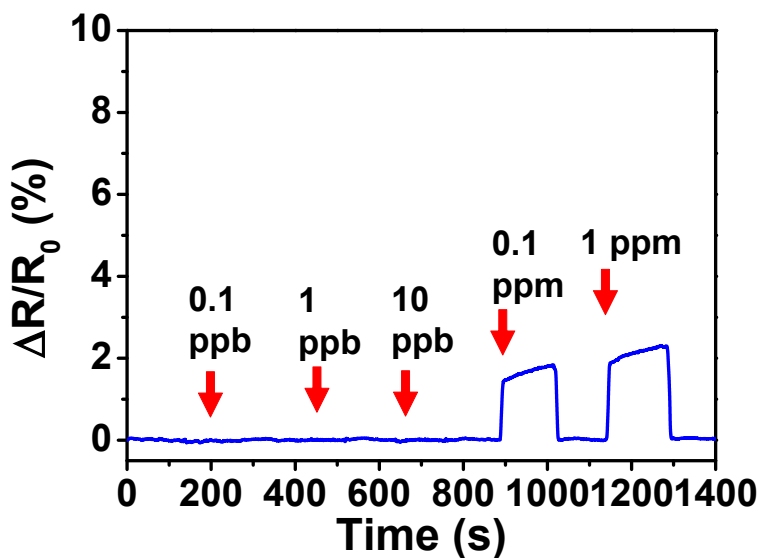


Fig. S16. Real-time responses of the PPy@SnO₂ nanoparticles upon periodic exposure to dimethyl methylphosphonate (DMMP); 0.1 ppb to 1 ppm.

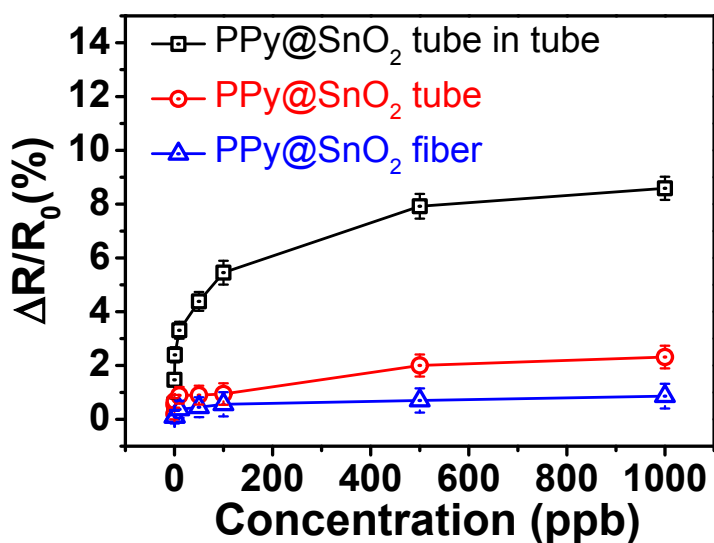


Fig. S17. Changes in sensitivity as a function of DMMP concentration calculated from the real-time responses.

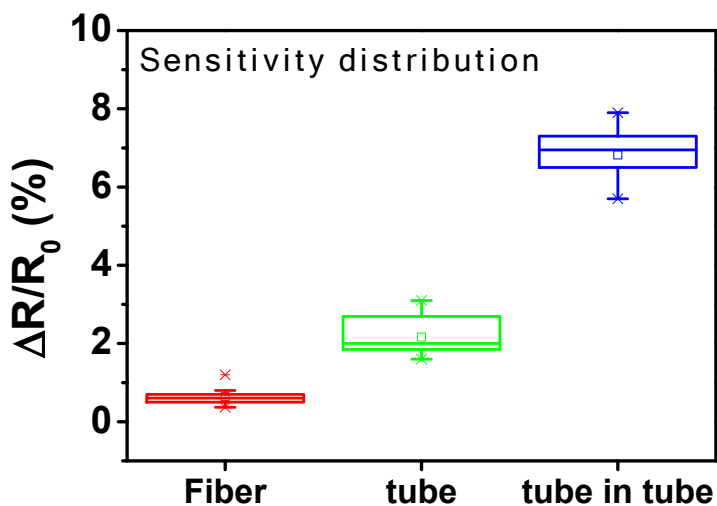


Fig. S18. Variation and comparison of the sensitivity parameter. These parameters were evaluated from 10 devices fabricated at 1 ppm